Vol. 35 (2004) ACTA PHYSICA POLONICA B No 12

PHYSICS OF PARTON SATURATION*

K. Golec-Biernat

H. Niewodniczański Institute of Nuclear Physics
Polish Academy of Sciences
Radzikowskiego 152, 31-342 Cracow, Poland

(Received November 17, 2004)

Basic ideas related to the description of a dense gluonic system in a nucleon, motivated by high energy scattering experiments at HERA and RHIC, are presented.

PACS numbers: 13.60 Hb

1. Introduction

The deep inelastic scattering experiments in which leptons probe nucleons with the help of electroweak bosons revealed the partonic structure of nucleons. In particular, the scaling behavior of the nucleon structure functions in the Bjorken limit found natural interpretation in terms of scattering on pointlike, spin 1/2 objects — partons. These are colored quarks of Quantum Chromodynamics (QCD). However, quarks carry only half of nucleon's longitudinal momentum. The missing half is provided by gluons to which the electroweak bosons do not directly couple. Thus, although not directly probed, gluons are extremely important for the description of the deep inelastic structure of nucleons. Quantitatively, this is summarized by the DGLAP evolution equations of QCD in which quark and gluon distributions are directly coupled. The sign of scaling violation, $\partial F_2/\partial \log Q^2$ at different values of the Bjorken variable x, is determined by a relative contribution of gluons to quarks. In the limit $x \to 0$, studied in the last ten years at HERA, the description of deep inelastic processes is dominated by strongly rising gluon distribution. Therefore, the small x limit corresponds to a study of a partonic system inside of a nucleon which is predominantly formed by gluons. The description of processes in such a system, as seen from the point of view perturbative QCD, is the aim of this presentation.

* Presented at the XLIV Cracow School of Theoretical Physics, Zakopane, Poland, May 28–June 6, 2004.

2. Strongly rising gluon distribution

The DGLAP evolution equations [1] predict strong rise of the gluon distribution in the double logarithmic limit, $x \to 0$ and $Q^2 \to \infty$, in which large logarithms $(\alpha_s \ln(1/x) \ln Q^2)^n$ have to be resumed [2],

$$xg(x,Q^2) \sim \exp\left\{ 2\sqrt{\overline{\alpha}_s \ln\frac{Q^2}{Q_0^2} \ln\frac{1}{x}} \right\}, \tag{1}$$

Here $\overline{\alpha}_s = N_c\, \alpha_s/\pi$, and $-Q^2$ equals virtuality of the photon probing a nucleon. Thus the gluon distribution rises stronger than any power of $\ln(1/x)$.

However, we are interested in the Regge limit of DIS, studied intensively at HERA, when $x \to 0$ and Q^2 is fixed. In this limit the center-of-mass energy of the $\gamma^* p$ system $\sqrt{s}$ goes to infinity since $x = Q^2/s$. The Regge limit in QCD relies on resummation of large logarithms $(\alpha_s \ln(1/x))^n$ for not too large (although perturbative) Q^2. The result is given in terms of the BFKL equation [3] which leads to the *unintegrated* gluon distribution rising as a power of x

$$f\left(x, k_T^2\right) \sim x^{-\lambda} \sqrt{k_T^2}\, \frac{\exp\left\{ -\ln^2\left(\frac{k_T^2}{k_0^2}\right) \Big/ D \right\}}{\sqrt{\pi D}}, \tag{2}$$

where $\lambda = 4\alpha_s \ln 2$ is the intercept of the famous BFKL pomeron, k_T is the gluon transverse momentum and $D = 2\overline{\alpha}_s \zeta(3) \ln(1/x)$ is the diffusion coefficient. Using a typical value of $\alpha_s = 0.2$, one finds $\lambda \simeq 0.5$. The gluon distribution from the DGLAP equations is obtained after the integration over the transverse momentum

$$xg\left(x, Q^2\right) = \int^{Q^2} \frac{dk_T^2}{k_T^2}\, f\left(x, k_T^2\right). \tag{3}$$

It is easy to see that in the BFKL approach $xg \sim x^{-\lambda}$, thus the integrated gluon distribution rises faster with decreasing x than in the double logarithmic limit. The same is true for the structure functions computed with the help of the k_T-factorization formula [4] in which the unintegrated gluon distribution is a crucial ingredient. Therefore, at small x, the nucleon structure function

$$F_2 \sim x^{-\lambda}. \tag{4}$$

Such a behavior cannot continue too far with decreasing x since ultimately it violates Froissart bound for $\gamma^* p$ scattering

$$F_2 \le c \ln^2\left(\frac{1}{x}\right), \tag{5}$$

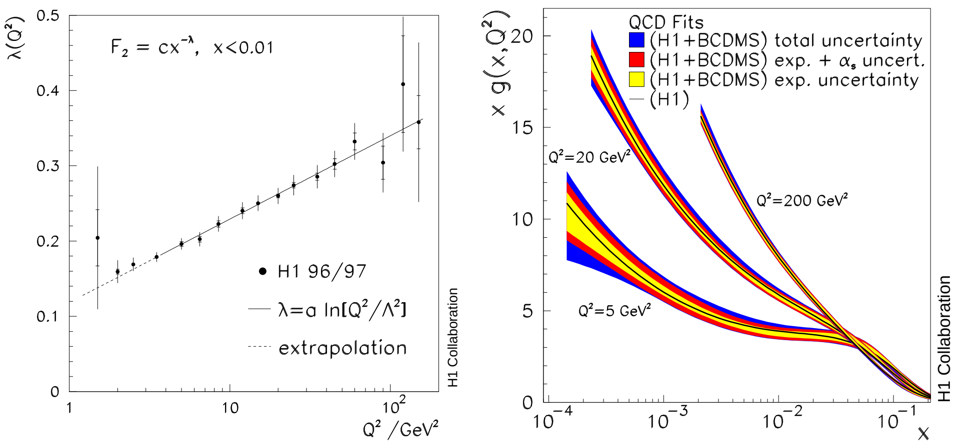

Fig. 1. The slope $\lambda(Q^2)$ in Eq. (4) and the corresponding gluon distributions from the DGLAP fits. The bands indicate uncertainty in the gluon determination.

written in analogy to hadronic reactions. Thus, the BFKL approach has be supplemented by unitarity corrections which change the power-like behavior into the logarithmic one.

The intercept of the BFKL pomeron does not depend on Q^2, however the data on F_2 from HERA can be parameterized at $x < 0.01$ using the form (4) with the Q^2-dependent slope $\lambda(Q^2)$, see Fig. 1 reproduced from [5]. In the QCD approach, $F_2(x, Q^2)$ in the DIS region can be described through a fit of initial parton distributions for the DGLAP evolution equations. As a result, a strongly rising gluon distribution is found, shown in Fig. 1 for several values of Q^2. These results can be interpreted as a manifestation of the double logarithmic limit (1) [6]. Thus, it seems that unitarity corrections are not needed at least for $Q^2 > 2$ GeV^2 and $x > 10^{-4}$. Moreover, the BFKL approach is not necessary for F_2 since the standard DGLAP based fits are flexible enough to describe data. There are, however, exclusive processes in which the BFKL configuration for the gluonic radiation is enhanced. These are forward jet production in DIS [7] or photoproduction of J/ψ mesons for large momentum transfer t [8]. Summarizing 10 years of running HERA, it was proven beyond any doubt that the small x limit of DIS is dominated by large gluon distributions. The question of the DGLAP *versus* BFKL gluon radiation schemes or the problem of unitarization corrections appeared to be more subtle than expected. Quite often the same class of data can be equally well described using different approaches, and there is no compelling evidence that one or the other resummation scheme, rooted in perturbative QCD, is exclusively visible in the data.

3. Parton saturation and geometric scaling

We will present an approach to the description of DIS at small x, alternative to that based on the DGLAP evolution equation and leading twist collinear factorization formulae. We assume from the very beginning that resummation of large logarithms $\ln(1/x)$ in such a way that unitarity is preserved is a crucial factor in the perturbative QCD description.

This is a vast subject initiated by Gribov, Levin and Ryskin in [9], where a non-linear correction to the DGLAP equation for the gluon distribution was introduced in the double logarithmic limit

$$\frac{\partial^2\, xg\left(x, Q^2\right)}{\partial \ln\left(\frac{1}{x}\right)\, \partial \ln\left(\frac{Q^2}{\Lambda^2}\right)} = \overline{\alpha}_{\rm s}\, xg\left(x, Q^2\right) - \frac{\alpha_{\rm s}^2}{R^2 Q^2}\Big[xg\left(x, Q^2\right)\Big]^2. \tag{6}$$

In the above the parameter R controls the strength of the nonlinearity. Physically, in the t-channel gluon exchange picture, the nonlinear term on the r.h.s. describes fusion of gluons (summation of fan diagrams) in addition to gluon emissions described by the linear term. With such a modification, the gluon distribution saturates with decreasing x, and so does the structure function. A more refined analysis of Mueller and Qiu [10] extends the GLR result by including nonlinear modifications for the sea quark distributions.

An important point in the gluon saturation approach is the x-dependent saturation scale $Q_{\rm s}^2(x)$. This is a value of Q^2 for a given x for which the non-linear term in Eq. (6) is comparable with the linear one:

$$xg\left(x, Q_{\rm s}^2\right)\, \frac{\alpha_{\rm s}(Q_{\rm s}^2)}{Q_{\rm s}^2} \simeq \pi R^2\,. \tag{7}$$

Therefore, saturation effects are important when the number of gluons xg times the elementary gluon–gluon interaction cross section $\alpha_{\rm s}/Q^2$ approaches the geometric size of the nucleon, or the gluonic system inside the nucleon. In such a case a simple additive treatment breaks down and gluons start to overlap. Form relation (7), $Q_{\rm s}^2 \sim xg$, thus the saturation scale rises with decreasing x. At small enough x, $Q_{\rm s}(x) \gg \Lambda_{\rm QCD}$ and the approach based on perturbative QCD is fully justified. The overall physical picture is presented in Fig. 2, in which different regions in the (x, Q^2)-plane are shown. Below the saturation scale line, where parton system is dilute, the linear evolution equations like DGLAP or BFKL apply. Close to the line, where the parton system becomes dense, the saturation corrections start to play an important role and nonlinear evolution equations appear. Thus, the saturation scale is an intrinsic characteristic of a dense gluon system.

The GLR equation (6) is a rather crude approximation because of the double logarithmic limit. The approach which we are going to present is based on a high energy factorization formula which goes beyond this limit.

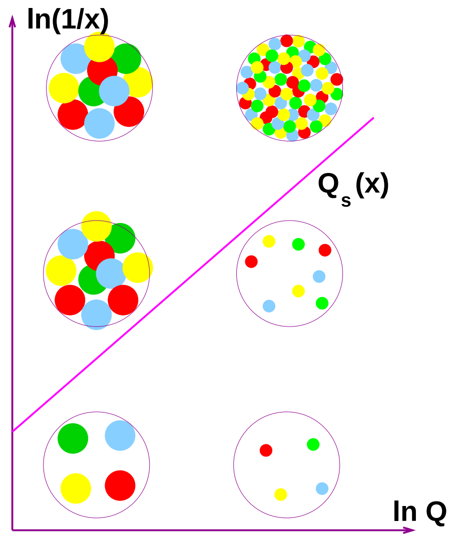

Fig. 2. Parton saturation in the (Q^2, x)-plane with the saturation scale.

It is well known that for high energy $\gamma^* p$ scattering, the correct degrees of freedom are given by $q\bar{q}$ colorless dipoles [11]. In the mixed representation, the transverse dipole size r and the longitudinal momentum fraction z with respect to the photon momentum are conserved in the high energy scattering, and [11]

$$F_2\left(x, Q^2\right) = \frac{Q^2}{4\pi^2 \alpha_{em}} \int d^2r\, dz \left| \Psi\left(r, z, Q^2\right) \right|^2 \sigma_{qq}(x, r)\,, \tag{8}$$

where $|\Psi|^2 \equiv |\Psi_{\rm T}|^2 + |\Psi_{\rm L}|^2$ involves known photon wave functions for transverse and longitudinal polarization. In the frame in which the virtual photon momentum q^+ is positive and large, $\Psi_{\rm T,L}$ describes the splitting of the virtual photon into a $q\bar{q}$ pair (dipole), and the dipole cross sections σ_{qq} describes the interaction of the dipole with the proton through multi-gluon exchanges, which dominate at small x. Details of this interaction have to be worked out from QCD or postulated based on general principles. In [12] the following form of σ_{qq} was proposed

$$\sigma_{qq}(x, r) = \sigma_0 \left(1 - \exp\left\{-r^2 Q_{\rm s}^2(x)\right\}\right), \tag{9}$$

which imposes the unitarity condition: $\sigma_{qq} \leq \sigma_0$ for large dipole sizes r. For small dipoles $\sigma_{qq} \to 0$, in agreement with the phenomenon of color transparency resulting from perturbative QCD. It is very important that the saturation scale $Q_{\rm s}^2(x)$, which sets the scale for the dipole size, was built in. Its form, $Q_s^2(x) = Q_0^2\, x^{-\lambda}$, together with the normalization σ_0 was successfully fitted to small x data on F_2, including the transition to photoproduction [13]. Having obtained the dipole cross section, it could be also applied to the description of DIS diffraction without tuning additional parameters [12]. In particular the constant ratio $\sigma_{\rm diff}/\sigma_{\rm tot}$ as a function of the total energy of the $\gamma^* p$ system was naturally explained. The unitarity condition imposed on σ_{qq} leads to $F_2 \sim c \ln(1/x)$, which fulfills the Froissart bound (5). Although such a behavior will never be tested at HERA, the presence of unitarity in the discussed approach allows for a unified treatment of inclusive and diffractive DIS data.

In the form (9) a very profound feature was encoded, the independent variables r and x are combined into one variable $rQ_s(x)$. A simple scaling argument leads to the conclusion that in the case of massles quarks, the $\gamma^* p$ cross section, $\sigma^{\gamma^* p} = (4\pi^2\alpha_{em}/Q^2)F_2$, is a function of only one variable [14]

$$\sigma^{\gamma^* p}\left(x, Q^2\right) = \sigma^{\gamma^* p}\left(\frac{Q^2}{Q_s^2(x)}\right). \tag{10}$$

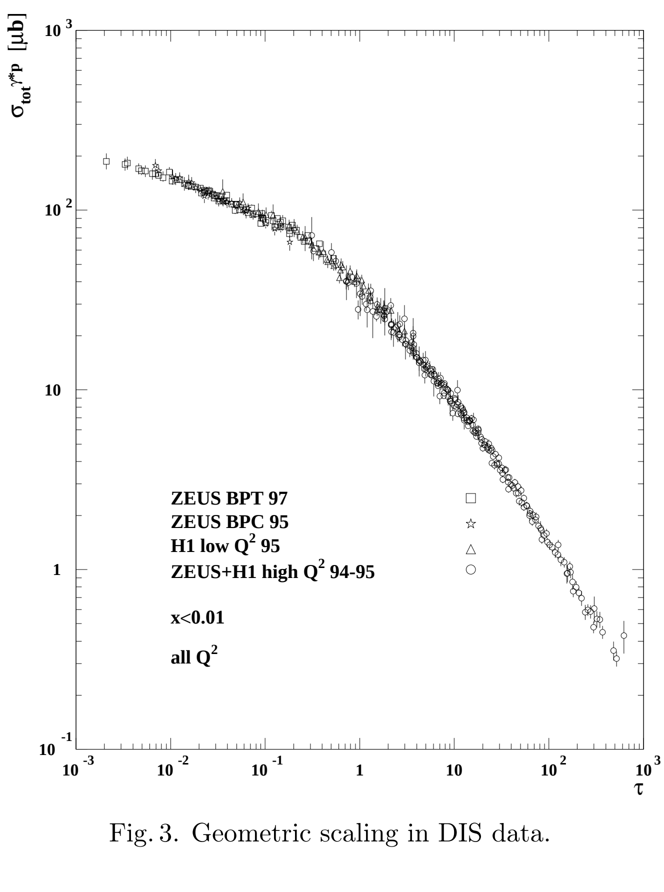

Fig. 3. Geometric scaling in DIS data.

This a phenomenon of geometric scaling in the small x data, resulting from the existence of the saturation scale and the scaling form of the dipole cross section (9). In Fig. 3 all DIS data with $x < 0.01$ were plotted against the scaling variable $\tau = Q^2/Q_s^2(x)$. As we see, to a good accuracy geometric scaling was found in the data from different experiments.

The natural question which arises here is how to combine the GLR idea of the gluon saturation with the presented model of DIS at small x in which the dipole degrees of freedom play the basic role.

4. Color glass condensate

The relation we are looking for is provided by Color Glass Condensate (CGC), an effective theory of low x gluons. In the s-channel approach to the high energy limit, the multigluon radiation encoded in the dipole cross section can be attributed to the virtual photon or the nucleon, depending on the frame of reference. In the frame in which most of the total energy is taken by the $q\bar{q}$ dipole, the gluon radiation is a part of the photon wave function. The parent dipole radiates soft ($z \ll 1$) gluons forming new dipoles (in the large N_c limit). In the frame in which most of the energy is taken by the nucleon (and the photon's momentum $q^+ > 0$), the gluon radiation is a part of the nucleon wave function, dominated by soft gluons. This part of the nucleon's wave function is described by CGC.

The CGC approach is based on the division of partons in a nucleon into fast and slow ones. The separation scale is given by $\Lambda^+ = xP^+$, where P^+ is fixed nucleon light-cone momentum. Partons with momenta $k^+ > \Lambda^+$ are fast, and partons with momenta $k^+ < \Lambda^+$ are slow. The fast partons are nearly frozen in light-cone time x^+, and serve as static color sources $\rho^a(x^-, \boldsymbol{x}_\perp)$ for slow partons [15]. The low x gluons are described by classical gauge fields A^a_μ, found after solving the Yang–Mills (Y–M) equations with the static sources. In order to compute a physical quantity which depends on soft modes, an average over color sources has to be calculated, *e.g.* for 2-point equal time correlation function

$$\left\langle A_\mu(x^+, \boldsymbol{x}_\perp) A_\nu(x^+, \boldsymbol{y}_\perp) \right\rangle_x = \int \mathcal{D}\rho\, W_x[\rho]\, A_\mu[\rho]\, A_\nu[\rho]\,, \tag{11}$$

where $A_\mu[\rho]$ is a solution of the Y–M equations with given color sources. The average involves some weight $W_x[\rho]$ which depends on an arbitrary separation scale Λ^+ (or the momentum fraction x). Lowering Λ^+, a part of slow partons becomes fast frozen sources. Thus, a renormalization group equation is derived for the weight $W_x[\rho]$, known as the JIMWLK equation, which is the basic equation of the CGC [16]

$$\frac{\partial W_x[\rho]}{\partial \ln\left(\frac{1}{x}\right)} = \frac{1}{2} \int\limits_{\boldsymbol{x}_\perp, \boldsymbol{y}_\perp} \frac{\delta}{\delta \rho^a(\boldsymbol{x}_\perp)}\, \chi_{ab}(\boldsymbol{x}_\perp, \boldsymbol{y}_\perp)\, \frac{\delta}{\delta \rho^b(\boldsymbol{y}_\perp)}\, W_x[\rho]\,. \tag{12}$$

This is a diffusion type equation with a positive definite kernel χ_{ab} which depends on the color sources via the Wilson line

$$V(\boldsymbol{x}_\perp) = P \exp\left\{ ig \int dx^- A^+(x^-, \boldsymbol{x}_\perp) \right\}\,. \tag{13}$$

In the above, $A^+[\rho]$ is a solution of the Yang–Mills equation in the covariant gauge: $\nabla_\perp^2 A^+ = -\rho$. Thus, the kernel χ_{ab} is highly nonlinear in the color charge density ρ. This is the reason why it is very difficult to find a general solution to the JIMWLK equation and various approximations have to be developed. Nevertheless, the gluon distribution was found in this approach in accordance with the GLR saturation ideas with the saturation scale. In the CGC the saturated gluons form a collective state described by strong classical color fields, $A^a \sim 1/g$, leading to highly nonlinear phenomena. In the weak field approximation, however, the linear BFKL equation is recovered.

Another important result concerns geometric scaling. Its domain of validity in the (x, Q^2)-plane was extended into the region where linear evolution equations with special boundary conditions hold [17]:

$$Q_{\rm s}^2(x) \,\le\, Q^2 \,\le\, \frac{Q_{\rm s}^4(x)}{\Lambda_{\rm QCD}^2}\,. \tag{14}$$

For more details, see the recent review [18] from which we reproduce an analogue of Fig. 1 with different domains in the (x, Q^2)-plane according to the CGC analysis.

5. Dipole cross section from CGC

The dipole cross section can be computed in the CGC approach from the relation

$$\sigma_{qq}(r, x) \,=\, 2 \int d^2b\,(1 - S(r, b, x))\,, \tag{15}$$

where the dipole scattering matrix $S(r, b, x)$ is an average of two Wilson lines

$$S(r, b, x) \,=\, \frac{1}{N_{\rm c}} \left\langle {\rm Tr}\,(V^\dagger(\boldsymbol{x}_\perp) V(\boldsymbol{y}_\perp)) \right\rangle_x\,. \tag{16}$$

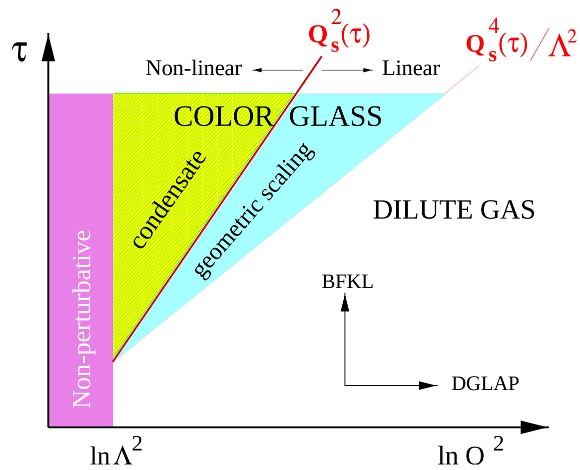

Fig. 4. Domains in the (x, Q^2)-plane according to CGC results. Here $\tau = \ln(1/x)$. Reproduced from [18].

Here the dipole size $r = \boldsymbol{x}_\perp - \boldsymbol{y}_\perp$, the impact parameter $b = (\boldsymbol{x}_\perp + \boldsymbol{y}_\perp)/2$, and trace is performed over color indices.

The JIMWLK equation written for the 2-point function (16) gives the equation derived for the first time by Balitsky [19]

$$\frac{\partial}{\partial Y}\Big\langle \mathrm{Tr}\,(V^\dagger_{\boldsymbol{x}}\,V_{\boldsymbol{y}})\Big\rangle_x = -\frac{\alpha_s}{2\pi^2}\int d^2\boldsymbol{z}\;\frac{(\boldsymbol{x}_\perp-\boldsymbol{y}_\perp)^2}{(\boldsymbol{x}_\perp-\boldsymbol{z}_\perp)^2\,(\boldsymbol{y}_\perp-\boldsymbol{z}_\perp)^2}$$
$$\times\Big\langle N_c\mathrm{Tr}\,(V^\dagger_{\boldsymbol{x}}\,V_{\boldsymbol{y}}) - \mathrm{Tr}\,(V^\dagger_{\boldsymbol{x}}\,V_{\boldsymbol{z}})\,\mathrm{Tr}\,(V^\dagger_{\boldsymbol{z}}\,V_{\boldsymbol{y}})\Big\rangle_x, \qquad (17)$$

where rapidity $Y = \ln(1/x)$. In order to solve this equation, an average of the 4-point function has to be known which in turn needs the knowledge of higher multi-point functions. In this way an infinite hierarchy of Balitsky's equations is obtained. However, a closed equation for the dipole scattering matrix is obtained in the large N_c limit in which the 4-point function factorizes

$$\Big\langle \mathrm{Tr}\,(V^\dagger_{\boldsymbol{x}}\,V_{\boldsymbol{z}})\,\mathrm{Tr}\,(V^\dagger_{\boldsymbol{z}}\,V_{\boldsymbol{y}})\Big\rangle_x \simeq \Big\langle \mathrm{Tr}\,(V^\dagger_{\boldsymbol{x}}\,V_{\boldsymbol{z}})\Big\rangle_x\Big\langle \mathrm{Tr}\,(V^\dagger_{\boldsymbol{z}}\,V_{\boldsymbol{y}})\Big\rangle_x. \qquad (18)$$

Thus Eq. (17) becomes

$$\frac{\partial}{\partial Y}S_{\boldsymbol{xy}} = \frac{\overline{\alpha}_s}{2\pi}\int d^2\boldsymbol{z}\;\frac{(\boldsymbol{x}_\perp-\boldsymbol{y}_\perp)^2}{(\boldsymbol{x}_\perp-\boldsymbol{z}_\perp)^2\,(\boldsymbol{y}_\perp-\boldsymbol{z}_\perp)^2}\,\left(S_{\boldsymbol{xz}}\,S_{\boldsymbol{zy}} - S_{\boldsymbol{xy}}\right), \qquad (19)$$

where we introduced the compact notation $S_{\boldsymbol{xy}} = S(r, b, x)$. An equivalent equation was derived by Kovchegov in the dipole approach for the amplitude $N = 1 - S$ [20]. A comprehensive discussion of properties of the Kovchegov equation is presented in [21]. At this point suffice it to say that in the b-independent case, the dipole cross section found from the solutions of Eq. (19) saturates to a constant value, similar to the phenomenological form (9). Moreover, the saturation scale and scaling behavior emerge, leading to geometric scaling for the DIS inclusive cross sections. The problem which appears for the Balitsky–Kovchegov equations is violation of the Froissart bound because of a power-like tail in b due to long-range contributions [22]. Thus, some phenomenological way of suppressing this tail, probably related to confinement effects, is necessary.

6. CGC and RHIC data

A significant effort was done to analyze RHIC data in terms of the CGC. The general picture of heavy ion scattering consists of three stages: the CGC formation followed by the quark–gluon plasma state which subsequently hadronizes. In this scenario, the CGC provides initial conditions for the quark–gluon plasma development, like in the hydrodynamical model of Hirano and Nara [23] applied to Au–Au collisions. However, the crucial assumption which has to be made is that gluons are thermalized at the initial moment of the hydrodynamical expansion. Gluon thermalization was studied in [24] with the conclusion that softer momentum modes ($k < Q_{\rm s}$), which dominate in the saturated system, thermalize fast enough through gluon number changing inelastic scattering processes..

Most of the produced particles at RHIC have low transverse momenta below 1 GeV, which is close to the value of the saturation scale estimated for RHIC. Therefore, it is tempting to interpret their rapidity spectra $dN/d\eta$ as a manifestation of rapidity distributions of the CGC gluons. In such a case parton–hadron duality has to be assumed. The analysis performed by Kharzeev, Levin and Nardi is based on the existence of the saturation scale in the gluon system with energy dependence taken from the analysis of HERA data. A good description of rapidity spectra was found [25].

Recently, new data on deuteron–gold collisions attracted a lot of attention. For this scattering, the final state effects are significantly reduced, and the initial state CGC effects might be more pronounced. The observed Cronin effect was qualitatively explained by the CGC [26]. In particular, enhancement of the nuclear modification factor at mid-rapidity and suppression at forward rapidities is a result of the nonlinear CGC evolution (17). Performed recently in [27] a detailed analysis of this phenomenon for d–Au collisions showed a very good agreement with the RHIC data. Also charged particle spectra were described.

The future searches of the CGC effects will concentrate on selected exclusive processes which are directly sensitive to the gluon distribution in the CGC. These could be photon and dilepton production or heavy quark production in the forward region in d–A collisions [28].

7. Summary

The studies of parton saturation reached full maturity. The enormous theoretical effort done in the last ten years, inspired by experimental results from HERA and RHIC, resulted in a well defined formulation of this phenomenon in terms of an effective QCD based theory, the Color Glass Condensate. Although still much work is needed to fully understand the CGC predictions, a specific combination of theoretical and experimental efforts ensures a lot of excitement in the years to come.

REFERENCES

[1] V.N. Gribov, L.N. Lipatov, *Sov. J. Nucl. Phys.* **15**, 438 (1972); G. Altarelli, G. Parisi, *Nucl. Phys.* **B126**, 298 (1977); Yu.L. Dokshitzer, *Sov. Phys. JETP* **46**, 641 (1977).

[2] A. De Rujula, S. L. Glashow, H. D. Politzer, S.B. Treiman, F. Wilczek, A. Zee, *Phys. Rev.* **D10**, 1649 (1974).

[3] L.N. Lipatov, *Sov. J. Nucl. Phys.* **23**, 338 (1976); E.A. Kuraev, L.N. Lipatov, V.S. Fadin, *Sov. Phys. JETP* **44**, 443 (1976); *Sov. Phys. JETP* **45**, 199 (1977); Ya.Ya. Balitsky, L.N. Lipatov, *Sov. J. Nucl. Phys.* **28**, 338 (1978).

[4] S. Catani, M. Ciafaloni, F. Hautmann, *Phys. Lett.* **B242**, 97 (1990); *Nucl. Phys.* **B366**, 657 (1991); J.C. Collins, R.K. Ellis, *Nucl. Phys.* **B360**, 3 (1991); E.M. Levin, M.G. Ryskin, Yu.M. Shabel'sky, A. Shuvaev, *Sov. J. Nucl. Phys.* **53**, 657 (1991).

[5] H1 Collaboration, C. Adloff *et al.*, *Phys. Lett.* **B520**, 183 (2001).

[6] R.D. Ball, S. Forte, *Phys. Lett.* **B335**, 77 (1994); *Phys. Lett.* **B335**, 77 (1994).

[7] H1 Collaboration, C. Adloff *et al.*, *Nucl. Phys.* **B538**, 3 (1999); *Phys. Lett.* **B462**, 440 (1999); ZEUS Collaboration, J. Breitweg *et al.*, *Eur. Phys. J.* **C6**, 239 (1999); *Phys. Lett.* **B474**, 223 (2000).

[8] H1 Collaboration, A. Aktas *et al.*, *Phys. Lett.* **B568**, 205 (2003).

[9] L.V. Gribov, E.M. Levin, M.G. Ryskin, *Nucl. Phys.* **B188**, 555 (1981); *Phys. Rep.* **100**, 1 (1983).

[10] A.H. Mueller, Jian-wei Qiu, *Nucl. Phys.* **B268**, 427 (1986).

[11] N.N. Nikolaev, B.G. Zakharov, *Z. Phys.* **C49**, 607 (1991); *Z. Phys.* **C53**, 331 (1992); A.H. Mueller, *Nucl. Phys.* **B415**, 373 (1994); *Nucl. Phys.* **B437**, 107 (1995).

[12] K. Golec-Biernat, M. Wüsthoff, *Phys. Rev.* **D59**, 014017 (1999); *Phys. Rev.* **D60**, 114023 (1999); *Eur. Phys. J.* **C20**, 313 (2001).

[13] J. Bartels, K. Golec-Biernat, H. Kowalski, *Phys. Rev.* **D66**, 014001 (2002).

[14] A.M. Staśto, K. Golec-Biernat, J. Kwieciński, *Phys. Rev. Lett.* **86**, 596 (2001).

[15] L.D. McLerran, R. Venugopalan, *Phys. Rev.* **D49**, 2233 (1994); *Phys. Rev.* **D49**, 3352 (1994); *Phys. Rev.* **D50**, 2225 (1994).

[16] J. Jalilian-Marian, A. Kovner, L. McLerran, H. Weigert, *Phys. Rev.* **D55**, 5414 (1997); J. Jalilian-Marian, A. Kovner, A. Leonidov, H. Weigert, *Nucl. Phys.* **B504**, 415 (1997); *Phys. Rev.* **D59**, 014014 (1999); H. Weigert, *Nucl. Phys.* **A703**, 823 (2002); E. Iancu, A. Leonidov, L. McLerran, *Nucl. Phys.* **A692**, 583 (2001); *Phys. Lett.* **B510**, 133 (2001); E. Ferreiro, E. Iancu, A. Leonidov, L. McLerran, *Nucl. Phys.* **A703**, 489 (2001).

[17] E. Iancu, K. Itakura, L. McLerran, *Nucl. Phys.* **A708**, 327 (2002); J. Kwieciński, A.M. Staśto, *Phys. Rev.* **D66**, 014013 (2002).

[18] E. Iancu, R. Venugopalan, `hep-ph/0303204`.

[19] I. Balitsky, *Nucl. Phys.* **B463**, 99 (1996).

[20] Y.V. Kovchegov, *Phys. Rev.* **D60**, 034008 (1999); *Phys. Rev.* **D61**, 074018 (2000).

[21] A.M. Staśto, *Acta Phys. Pol. B*, **35**, 0000 (2004), these proceedings.

[22] A. Kovner, U.A. Wiedemann, *Phys. Rev.* **D66**, 051502 (2002); *Phys. Rev.* **D66**, 034031 (2002); *Phys. Lett.* **B551**, 311 (2003); K. Golec-Biernat, A.M. Staśto, *Nucl. Phys.* **B668**, 345 (2003).

[23] T. Hirano, Y. Nara, *Nucl. Phys.* **A743**, 305 (2004).

[24] R. Baier, A.H. Mueller, D. Schiff, D.T. Son, *Phys. Lett.* **B502**, 51 (2001).

[25] D. Kharzeev, M. Nardi, *Phys. Lett.* **B507**, 121 (2001); D. Kharzeev, E. Levin, *Phys. Lett.* **B523**, 79 (2001).

[26] D. Kharzeev, Yu.V. Kovchegov, K. Tuchin, *Phys. Rev.* **D68**, 094013 (2003); J. Albacete, N. Armesto, A. Kovner C. Salgado, U. Wiedemann, *Phys. Rev. Lett.* **92**, 082001 (2004).

[27] D. Kharzeev, Yu.V. Kovchegov, K. Tuchin, `hep-ph/0405045`.

[28] D. Kharzeev, K. Tuchin, *Nucl. Phys.* **A735**, 248 (2004); J.P. Blaizot, F. Gelis, R. Venugopalan, *Nucl. Phys.* **A743**, 57 (2004).